Wireless Pers Commun (2014) 78:729–740
DOI 10.1007/s11277-014-1780-5

Diversity Antenna Design for Wireless Alarm Networks

Mustafa Murat Bilgiç · Korkut Yeğin

Published online: 22 April 2014

Abstract Printed circuit board antennas degrade considerably when the wireless node is placed on or near metallic surfaces. One such application is wireless alarm network where nodes are placed on a metallic fence. As wireless transmission is regarded as the most expensive operation in terms of sensor node energy, it is more than a necessity to have a good antenna design. We simulate the performances of typical printed circuit board (PCB) antennas with proximity to metallic fence and simulations show that traditional antenna structures exhibit poor performance for these applications. Instead, we propose a low-cost two-antenna diversity system that utilizes two PCB antennas with different radiation pattern coverage. Antenna diversity by means of radio frequency switches was implemented for two configurations: single state antenna selection and equal-gain diversity combination. Diversity gains were calculated for free-space and over-the-fence operating conditions, and the best antenna configuration is suggested for practical applications.

Keywords Antenna · Switch diversity · Wireless sensor networks · PCB antennas · Printed dipole

1 Introduction

In many applications of wireless sensor networks, small, low-power sensor nodes are desired. These nodes are usually equipped with printed circuit board (PCB) antennas. Often these antennas are designed to have omnidirectional radiation pattern. Indeed many reference antenna designs possess this property for free space radiation conditions. However, it is also well known that performance of PCB antennas is very prone to circuit board size and nearby components. Real life operating environment significantly alter the radiation pattern of the antenna which has been designed for free space applications. Especially, near metal or metal-like structures, antenna radiation pattern deteriorates significantly, and high power

M. M. Bilgiç · K. Yeğin (✉)
Department of Electrical and Electronics Engineering, Yeditepe University, Istanbul 34755, Turkey
e-mail: kyegin@yeditepe.edu.tr

transmission of the node becomes inevitable, which, in turn, drains more battery power. Near-ground sensors or sensors placed on metallic fences are just some common applications of these. In previous studies, it's been shown that wireless transmission is the most expensive operation in terms of wireless sensor node energy [1]. Therefore, a careful antenna design is more than a necessity but a requirement to reduce energy consumption. However, operating environment and physical size restrictions of sensor boards place severe limitations on the antenna design. Instead, one can consider multiple antenna use in selection diversity.

Switch diversity setting may be the least optimal among the existing diversity techniques, but it is the easiest to implement with little added cost to the sensor node. Antennas, however, must be carefully designed to minimize not only their mutual interaction, but also their overlapping angular coverage and correlation coefficient. In addition, real operating environment of the sensor nodes must be taken into consideration during the antenna design.

Instead of using two-antenna switch diversity, multiple antennas or antennas with parasitic elements can be designed for switched beam configuration [2–9]. Quad corner reflector, microstrip parasitic array, multi-element antenna arrays are some examples of these antennas. However, most of these antennas require much larger space than conventional designs, and therefore, they have very limited practical use.

In this study, we propose two-antenna system in a switch diversity setting to overcome these difficulties without significantly increasing the board size and complexity of the wireless node. Our goal is to enhance transmission/reception characteristics of the node in the direction where the radiation/reception is desired. We are particularly interested in sensor nodes on metallic fence. Hence, rather than omnidirectional or broadside coverage, we are interested in coverage along the metal fence to the right or to the left of the sensor board. We studied six different antenna configurations through 3D electromagnetic solver, and built two of these antennas for measurements. Antenna correlation coefficient and diversity antenna gains are also studied and presented.

2 Antenna Design

Typical over the fence WSN application is shown in Fig. 1. Wireless sensor nodes are placed in proximity to fence (<10 cm) and are separated by approximately 10 m. Vibration sensors are inside the boxes to detect the presence of disturbance (intruder) on the fence. When the sensor board is close to this metallic surface, the antenna characteristics get affected considerably. Therefore, we placed two antennas on the wireless node sensor board and studied antenna performance for this particular application. Our goal is to deduce the optimal antenna shape among traditional antenna structures that would have the best communication link between the two neighboring nodes for over-the-fence WSN applications. In addition, all antennas must satisfy the impedance bandwidth requirement of $|S_{11}| < -7.5$ dB.

We first took an inverted-F antenna utilized in Texas Instruments Inc. (TI) sensor boards [10]. Although inverted-F's are known to have narrow bandwidth, TI's design is very robust and covers the entire 2.4 GHs ISM band. Other attractive parts of the TI's design are its good radiation pattern coverage, less variation in gain as frequency changes, and its relatively small form factor compared to its counterparts. These attributes make TI antenna as prime choice for the designers. However, an antenna placed close to metallic surface creates a null along the symmetry axis with its image. Thus, communication devices placed closed to metallic surface experience major difficulties for establishing seamless communication. In the case of metallic fence, the situation even gets worse as metallic grids distort the pattern by not only creating a gain minima along fence surface but also tilt the beam to undesired directions. The

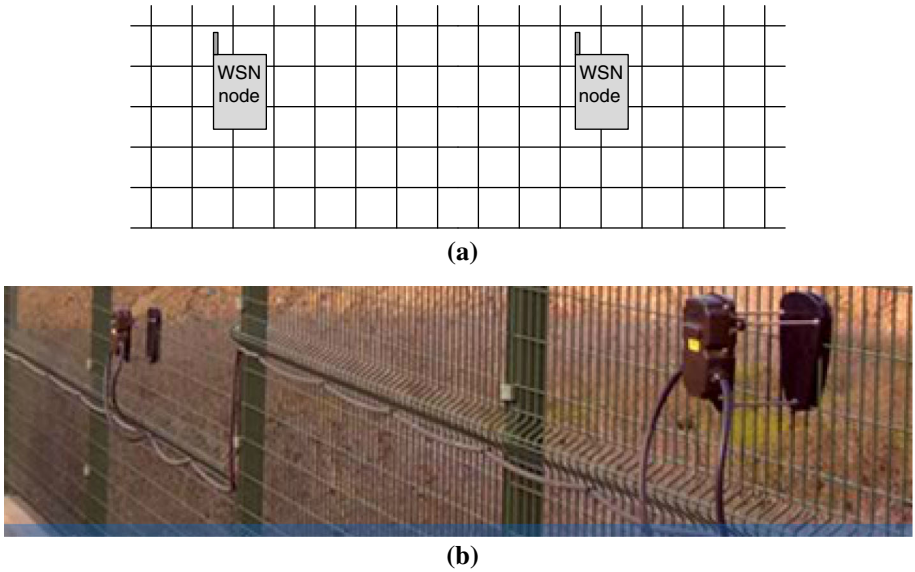

Fig. 1 Over the fence alarm network application of WSN, **a** simulation model, **b** field application (Courtesy of Genetlab Inc.)

grids are in the order of operation wavelength and are not electrically small enough to be considered like a metal. Therefore, present application is even worse than placing antenna close to metallic surface. Careful and extensive simulations of the antenna with the fence are required. A straightforward determination of which antenna structure works best is to measure the antenna radiation patterns on the fence. However, this is almost impossible in an indoor antenna measurement system as the size of the fence is quite large. Instead one can consider calibrated outdoor antenna measurement ranges, but these are scarce and usually reserved for automotive and military testing. Thus, simulations play a critical role in determination of antenna structures for this particular application.

Starting with TI's reference design, we placed two antennas in parallel and perpendicular to each other as shown in Fig. 2. In parallel orientation, we hoped to cover complementary patterns relative to sensor node, whereas in perpendicular orientation, we expected to receive both polarizations if either one of the polarization was not matched to the antenna polarization. We implemented the same reasoning with a printed dipole antenna as illustrated in Fig. 3. Marchand balun was also implemented with the dipole to alleviate the effects of unbalanaced currents on the antenna due to fence loading and the PCB ground. Balanced antennas are usually less prone to environmental changes and nearby structures. Lastly, we took wire monopole perpendicular to PCB as this type of antenna is very common in many applications though hardly optimal in many applications. To decrease the increased height of the sensor board, we also considered an inclined monopole for the study (Fig. 4).

All six antennas were modeled using FEKO (3D electromagnetics field solver) with the metallic fence. Although FEKO utilizes integral equation based Method of Moments solver and is ideal for free space radiation simulations, presence of metallic fence drastically increases the computational burden. The metallic fence whose wire dimensions were less than one fifth of wavelength at 2.45 GHz, (i.e. around 10 mm) had dimensions 10m length and 1m width where the wires were placed with 10 cm intervals in both horizontal and vertical

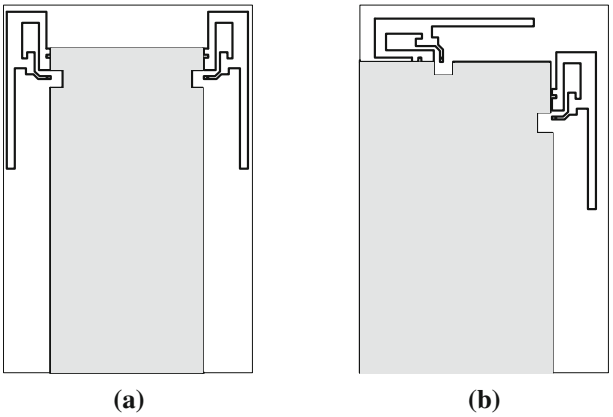

Fig. 2 Inverted F (Texas Instruments reference design), **a** parallel, **b** perpendicular configurations (dimensions from [10])

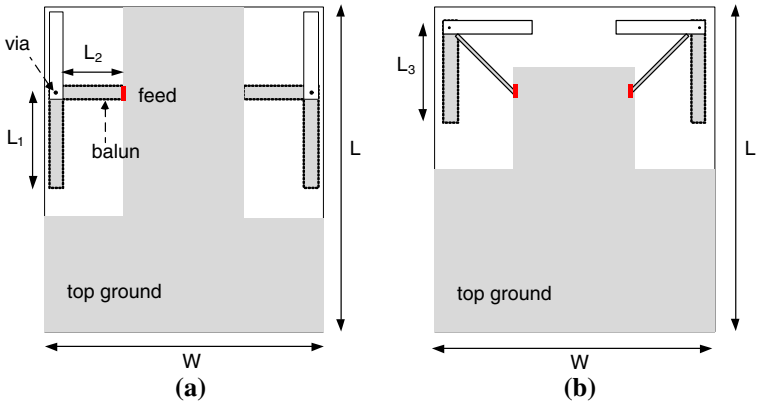

Fig. 3 Printed dipole antenna with balun, a) parallel, b) perpendicular configuration ($L_1 = 23.5$ mm, $L_2 = 17.8$ mm, $L_3 = 20.3$ mm L= 70 mm, W=60 mm)

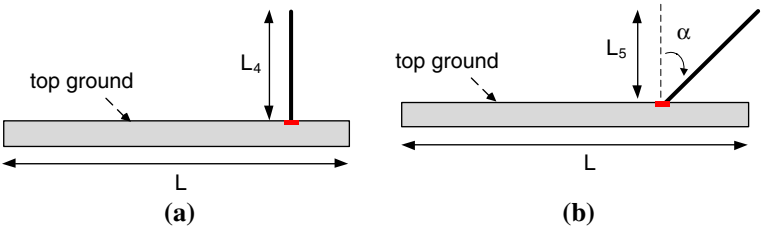

Fig. 4 Monopole on PCB, **a** vertical, **b** inclined ($L_4 = 29.5$ mm, $L_5 = 15.2$ mm, $\alpha = 60°$)

directions. Wire grids were of square type. When two over-the-fence wireless sensor nodes are separated by 10 m, the signal coupling between the transmit and receive nodes placed on the fence is calculated using scattering parameters (S-parameters) together with the average gain in the 2.4–2.5 GHz frequency band. The results are presented in Table 1. To ensure that the simulated results do not reflect a particular spacing or separation, a simple perturbation

Table 1 Simulation results of antennas

	Average Gain (dBi)	S_{21} (dB) @2.45 GHz
Printed dipole antenna (parallel)	4.8	−55
Printed dipole antenna (perpendicular)	1.06	−73
Inverted F antenna (parallel)	2.07	−62
Inverted F antenna (perpendicular)	1.92	−75
Vertical monopole	1.05	−63.5
Inclined monopole	1.27	−63

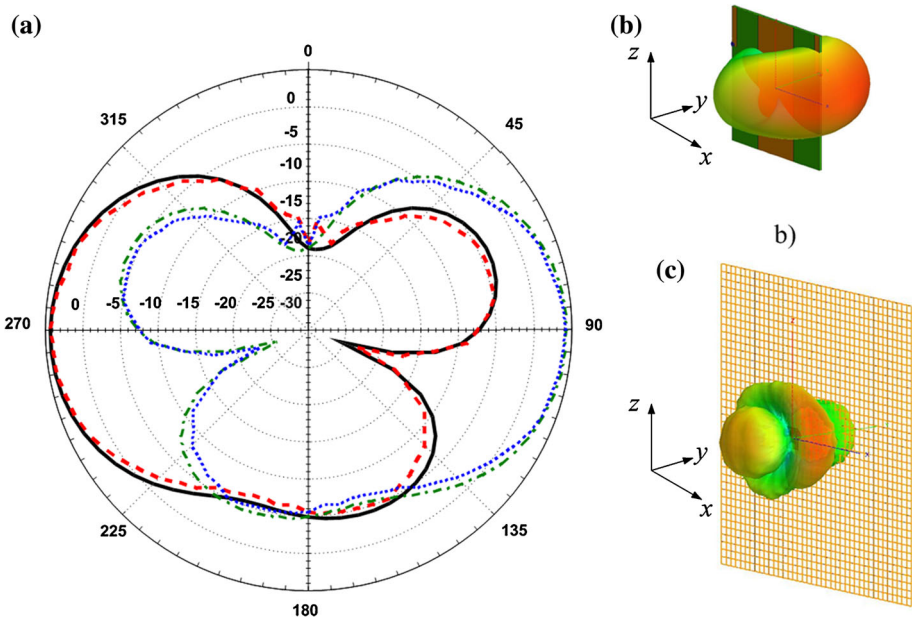

Fig. 5 **a** Simulated radiation pattern for dipole antenna pair on $x - z$ plane (*black solid line* Dipole in free space port 1 excited, *red dashed line* Dipole in front of fence, port 1 excited, *green dashed with dotted line* Dipole in free space port 2 excited, *blue thick dashed line* Dipole in front of fence, port 2 excited) **b** Simulated 3D pattern of dipole pair in free space (single port excited). **c** Simulated 3D pattern of dipole pair in front of the fence (single port excited). (Color figure online)

analysis was performed by displacing the antenna 2 cm closer and farther from the fence and displacing the receive antenna by 5 cm apart and closer to the transmit antenna. No significant changes were observed and the same analysis was carried out with 4 cm on antenna location with respect to fence and 10 cm with respect to each other. Simulation results revealed that printed dipole in parallel configuration exhibited the best performance. Next possible candidate was inverted-F in parallel configuration.

Simulated radiation patterns and impedances were analyzed for printed dipole and inverted-F. The radiation patterns and gain for parallel printed dipole are shown in Figs. 5 and 6, respectively. Gain and radiation patterns of printed dipole are compared to those of free-space conditions to understand the extent of change in antenna characteristics. Presence of metallic fence does not significantly alter the maximum gain, but it definitely impacts the

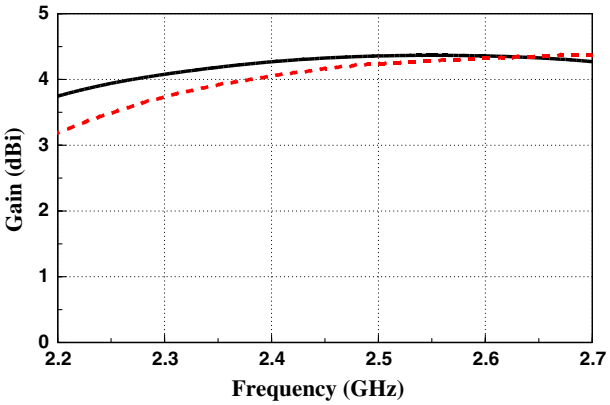

Fig. 6 Simulated gain on $x - y$ plane of dipole antenna. (*black solid line* Dipole in free space, *red dashed line* Dipole in front of fence). (Color figure online)

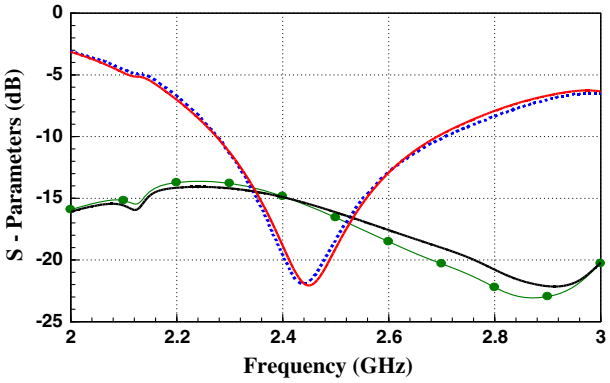

Fig. 7 Simulated S–parameters versus frequency plot for Dipole antenna pair. (*red solid line* S_{11} magnitude in free space, *thick black solid line* S_{21} magnitude in free space, *blue thick dashed line* S_{11} magnitude in front of fence, *green bullet series* S_{21} magnitude in front of fence). (Color figure online)

radiation patterns. Nevertheless, the antenna had directional pattern towards the side where the antenna was placed, which was the main motivation behind this configuration.

The S-parameters of printed dipole are shown in Fig. 7. Presence of metallic fence does not significantly change the S-parameters (impedance match and transmission/reception) of printed dipole due to its balanced nature.

We carried out a similar analysis for inverted-F parallel configuration antenna for over-the-fence and free-space conditions. The results are shown in Figs. 8 and 9.

It is obvious that inverted-F gets considerably affected from the presence of metallic fence. Although post tuning have been performed to optimize antenna performance for metallic fence presence, its gain and radiation pattern are very different than its free-space counterpart.

Antenna simulations with antennas placed on metallic fence revealed that printed dipole with integrated balun in parallel configuration produced superior results for two-antenna diversity system.

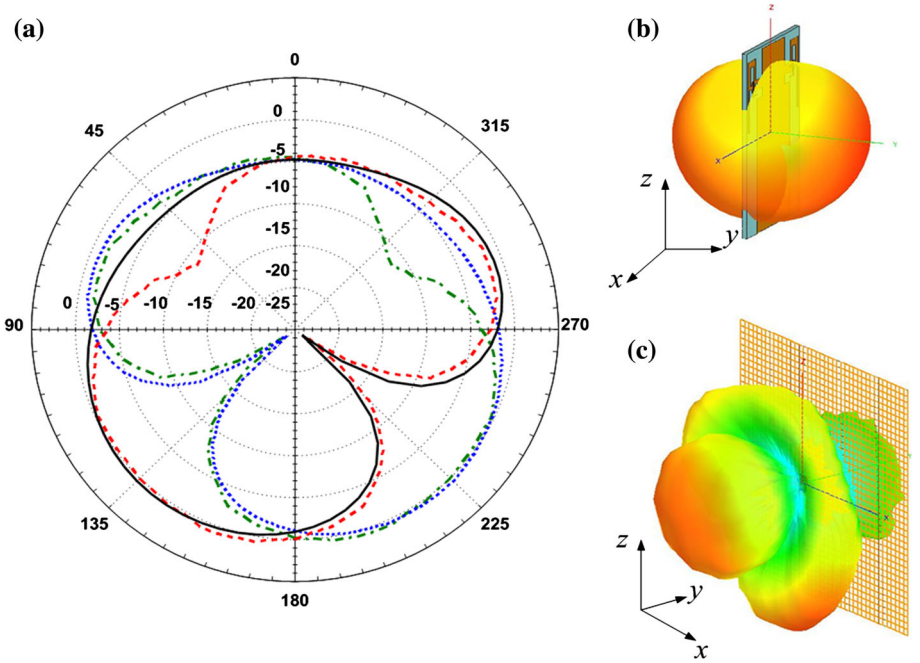

Fig. 8 **a** Simulated radiation pattern for inverted-F antenna pair on $x - z$ plane (*black solid line* Inverted-F in free space port 1 excited, *red dashed line* Inverted-F in front of fence, port 1 excited, *green dashed with dotted line* Inverted-F in free space port 2 excited, *thick blue dashed line* Inverted-F in front of fence, port 2 excited) b) Simulated 3D pattern of inverted-F pair in free space (single port excited). c) Simulated 3D pattern of inverted–F pair in front of fence (single port excited). (Color figure online)

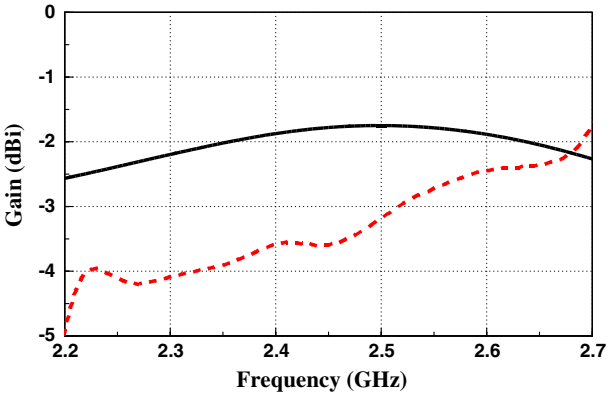

Fig. 9 Simulated gain on $x - y$ plane for inverted-F antenna (*black solid line* inverted–F in free space, *thick red dashed line* inverted-F in front of the fence). (Color figure online)

3 Antenna Diversity

To assess the performance gained by using two antennas, the correlation between the antennas is studied first. Diversity gain of a two-antenna system can be defined as

$$G_{div} = \frac{P_{div}}{P_{single}} \tag{1}$$

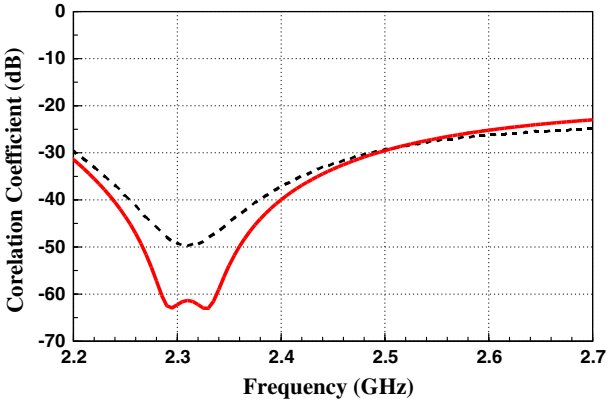

Fig. 10 Calculated envelope correlation coefficient for printed dipole antenna pair. (*red solid line* ρ_e in free space, *black dashed line* ρ_e in front of fence). (Color figure online)

where P_{div} is the power level after diversity combining, P_{single} is the power level at the single antenna, and both power levels are read at the same cumulative distribution function value [11,12]. If P_{single} is replaced with that of an ideal single antenna with 100 % efficiency, the diversity gain is called effective diversity gain. The envelope correlation for a two-antenna system can be stated as [13]

$$\rho_e = \frac{\left| \iint \left[\vec{F}_1(\theta,\varphi) \cdot \vec{F}_2(\theta,\varphi) \right] d\Omega \right|^2}{\left(\iint \left| \vec{F}_1(\theta,\varphi) \right|^2 d\Omega \right) \left(\iint \left| \vec{F}_2(\theta,\varphi) \right|^2 d\Omega \right)} \tag{2}$$

where $\vec{F}_i(\theta,\varphi)$ is the radiation pattern of the antenna system when ith antenna is excited and the port is terminated with matched load, and "$\cdot$" denotes complex Hermitian product. It is possible to express ρ_e in terms of S-parameters of the two-antenna system as:

$$\rho_e = \frac{\left| S_{11}^* S_{12} + S_{21}^* S_{22} \right|^2}{\left(1 - \left(|S_{11}|^2 + |S_{21}|^2\right)\right)\left(1 - \left(|S_{22}|^2 + |S_{12}|^2\right)\right)} \tag{3}$$

When $\rho_e \leq 0.5$ and almost equal power levels appear at the terminals of the both antenna, diversity gain can be achieved. In a typical selection diversity application, minimum ρ_e will result in maximum diversity gain [3,14–16]. Envelope correlation coefficients for parallel printed dipoles using simulated S-parameters are shown in Fig. 10 for free-space and over the fence conditions. The envelope correlation coefficient is very low over the entire operation band. Coupling can occur through free space and through ground currents as they share common ground. Although the physical separation between the antennas is about $0.45\lambda_o$ where λ_o represents the free space wavelength, the coupling is very small due to balanced nature of the antennas.

Complex correlation coefficient can be expressed in terms of envelope correlation coefficient as:

$$|\rho_s| = \sqrt{\rho_e}. \tag{4}$$

On the other hand, apparent diversity gain (G_{app}) can be approximated as

$$G_{app} = 10\sqrt{1 - |\rho_s|^2}, \tag{5}$$

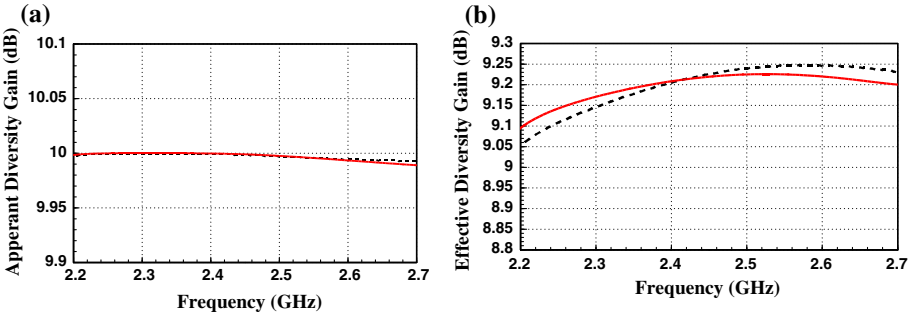

Fig. 11 Diversity gains, **a** apparent diversity gain (*red solid line* G_{app} in free space, *black dashed line* G_{app} in front of fence.), **b** effective diversity gain (*red solid line* G_{eff} in free space, *black bullet series* G_{eff} in front of fence). (Color figure online)

and effective diversity gain becomes

$$G_{eff} = \eta_{rad} G_{app} \tag{6}$$

where η_{rad} is radiation efficiency. Diversity gains for printed dipole using simulation results are displayed in Fig. 11. It can be seen that presence of metallic fence did not impact diversity gains as free-space and over the fence simulations are very close to each other. This is expected as the radiation pattern of the dipole antenna was not considerably affected by the fence as illustrated in Fig. 5.

The block diagram of the two-antenna diversity system with single switch and dual-switch are shown in Fig. 12. In single switch mode, either antenna A or antenna B is selected. In dual-switch mode either single A or single B or A-B together can be selected. First switch determines which of the mode will be selected between single modes (A or B). If microcontroller selects two-antenna together mode, then first switch is not necessary for the rest of the operation, and received signal strength indicator (RSSI) level for the measurement is the average of the both of the antennas. Radio frequency (RF) output of the first switch is also a RF input for switch 2. RF switch, AS214-92LF is used in the configurations. It is selected for its low insertion loss (0.4 dB), low DC power consumption and good isolation (26 dB) at 2.4 GHz.

4 Measurements

Prototypes were built on 1.56 mm thick FR4 substrate material with 1oz copper. The antenna measurements were carried out to validate the simulation results of S-parameters. The pictures of the prototypes are shown in Fig. 13. Measurements were carried out with network analyzer (Rohde & Schwarz ZVA-40). Measured S-parameters for printed dipole and inverted-F are shown in Figs. 14 and 15. They exhibited good match within the frequency band of interest. Moreover, measured coupling between the antennas were very low as evidenced in simulations. There is an apperant frequency shift in impedance match of printed dipole to higher frequencies and to lower frequencies for inverted-F antenna. Although both are below −10 dB match within the frequency band of interest, we attribute this discrepancy to variation in the dielectric constant of FR4 substrate. Antenna radiation patterns were not measured as it would require a large indoor anechoic chamber or a calibrated outdoor measurement facility, which are scarce.

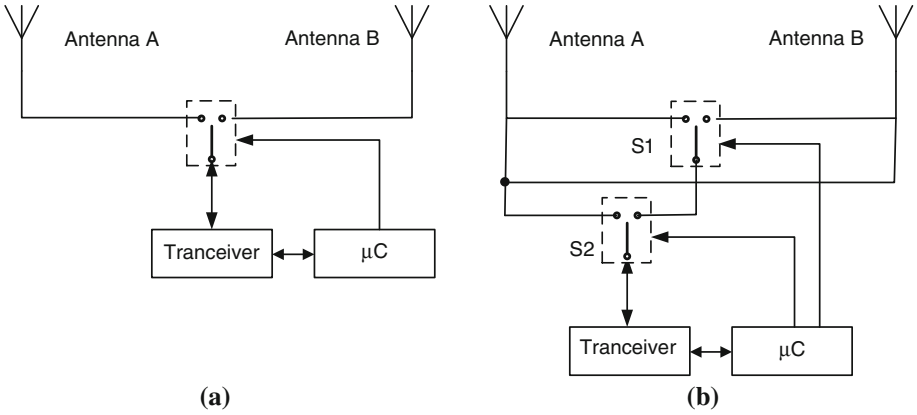

Fig. 12 Antenna diversity, **a** single switch, **b** dual-switch (three modes)

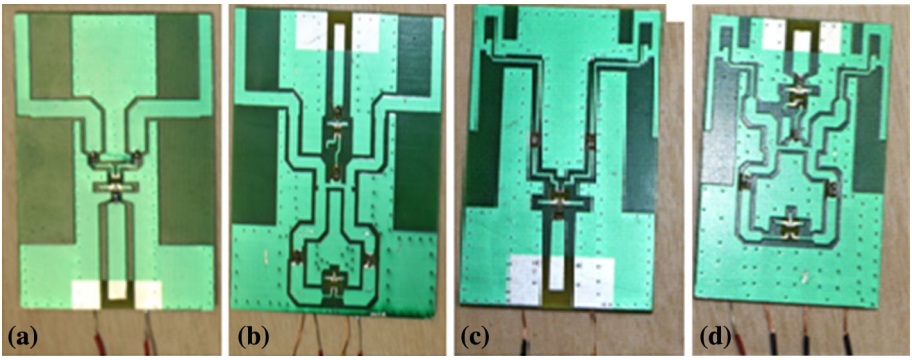

Fig. 13 Prototypes of antennas **a** printed dipole top layer, **b** printed dipole bottom layer, **c** inverted-F top layer, **d** inverted-F bottom layer

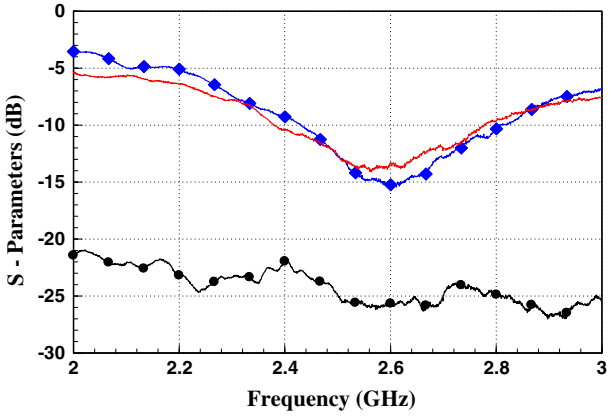

Fig. 14 Measured S–parameters for printed dipole antenna pair (*red solid line* S_{11} magnitude, *black bullet series* S_{21} magnitude, *blue diamond line* S_{22} magnitude). (Color figure online)

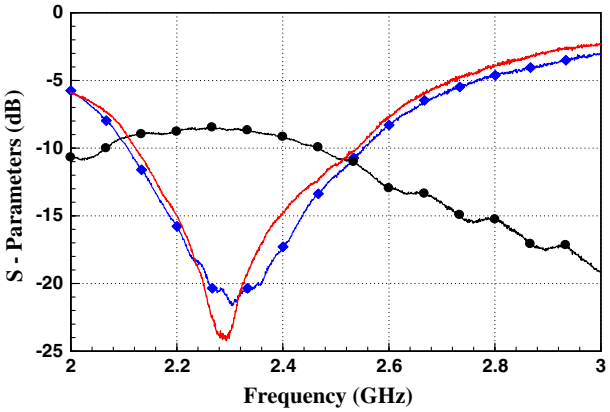

Fig. 15 Measured S–parameters for inverted-F antenna pair (*red solid line* S_{11} magnitude, *black bullet series* S_{21} magnitude, *blue diamond line* S_{22} magnitude). (Color figure online)

5 Conclusions

Wireless node antennas for over-the-metallic fence application of WSN are studied with two-antenna configuration. Antenna types and locations on PCB board are investigated for antenna performance in terms of S-parameters and gain. For pattern diversity, antennas placed on opposite sides of the PCB had better characteristics. Using simulations, six different antenna configurations were compared to each other, and only two were further analyzed for reception and diversity implementation. Among the traditional antenna structures, balanced printed dipole antenna with integrated PCB balun exhibited superior performance in simulations. Diversity gains were calculated using envelope correlation coefficient. Switch diversity system with single switch where either one of the antennas can be selected or dual-switch configuration where both antennas combined for equal gain diversity is also proposed for WSN over the fence applications.

References

1. Anastasi, G., Conti, M., Francesco, M., & Passarella, A. (2009). Energy conservation in wireless sensor networks: A survey. *Ad Hoc Networks*, *7*(3), 537–568.
2. Dietrich, C. B, Jr, Dietze, K., Nealy, J. R., & Stutzman, W. L. (2001). Spatial, polarization, and pattern diversity for wireless handheld terminals. *IEEE Transactions on Antennas and Propagation*, *49*(9), 1271–1281.
3. Foschini, G. J., & Gans, M. J. (1998). On limits of wireless communications in a fading environment when using multiple antennas. *Wireless Personal Communications*, *6*, 311–335.
4. Leather, P. S. H., & Parsons, D. (2003). Antenna diversity for UHF hand portable radio. *Electronics Letters*, *39*(13), 946–948.
5. Chang, D.-C., Zeng, B.-H., & Liu, J.-C. (2009). Reconigurable angular diversity antenna with quad corner reflector arrays for 2.4 GHz applications. *IET Microwaves, Antennas & Propagation*, *3*(3), 522–528.
6. Lai, M.-I., Wu, T. Y., Hsieh, J. C., Wang, C. H., & Jeng, S. K. (2008). Compact switched-beam antenna employing a four-element slot antenna array for digital home applications. *IEEE Transactions on Antennas and Propagation*, *56*(9), 2929–2936.
7. Zhang, S., Hu, G. H., & Bernhard, J. T. (2004). A pattern reconfigurable microstrip parasitic array. *IEEE Transactions on Antennas and Propagation*, *52*(10), 2773–2776.

8. Giorgetti, G., Cidronali, A., Gupta, S. K. S., & Manes, G. (2007). Exploiting low-cost directional antennas in 2.4 GHz IEEE 802.15.4 wireless sensor networks. In *Proceedings of the 10th European Conference on Wireless Technology*.
9. Luca, C., Guglielmi, S., Patrono, L., & Tarricone, L. (2013). Switched beam antenna for wireless sensor network nodes. *Progress in Electromagnetics Research C*, *39*, 193–207.
10. http://www.ti.com/lit/an/swru120b/swru120b.pdf Last accessed Feb 25th, 2014.
11. Kildal, P.-S., Rosengren, K., Byun, J., & Lee, J. (2002). Definition of effective diversity gain and how to measure it in a reverberation chamber. *Microwave and Optical Technology Letters*, *34*(1), 56–59.
12. Taga, T. (1990). Analysis for mean effective gain of mobile antennas in land mobile radio environments. *IEEE Transactions on Vehicular Technology*, *39*(2), 117–131.
13. Blanch, S., Romeu, J., & Corbella, I. (2003). Exact representation of antenna system diversity performance from input parameter description. *Electronics Letters*, *39*(9), 705–707.
14. Kildal, P.-S., & Rosengren, K. (2003). Electromagnetic analysis of effective and apparent diversity gain of two parallel dipoles. *IEEE Antennas and Wireless Propagation Letters*, *2*, 9–13.
15. Kong, N., & Milstein, L. B. (1999). Average SNR of a generalized diversity selection combining scheme. *IEEE Communications Letters*, *3*(3), 57–59.
16. Kong, N., & Milstein, L. B. (2000). SNR of generalized diversity selection combining with nonidentical rayleigh fading statistics. *IEEE Transactions on Communications*, *48*, 1266–1271.

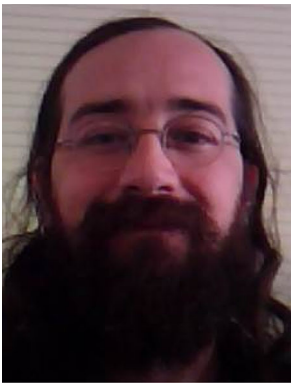

Mustafa Murat Bilgiç received BS and MS degrees in Electrical and Electronics Eng., Yeditepe University, Istanbul, Turkey in 2002 and 2008. He is currently pursuing his Ph.D degree. His main research interests are phased array antennas, wideband antennas, and sensor networks.

Korkut Yeğin obtained his B.S. degree in Electrical and Electronics Engineering from Middle East Technical University, Ankara, Turkey, M.S. degree in Electrical and Computer Engineering, M.S. degree in Plasma Physics, and Ph.D. degree in Electrical and Computer Engineering at Clemson University, SC, in 1992, 1996, 1998, and 1999, respectively. His research interests include wideband antennas, RF and microwave circuits, and UWB radar. He worked as a post-doctoral fellow at the University of Illinois Urbana-Champaign from 2000 to 2002, and as an Advanced Development Engineer at Delphi Delco Electronics, MI from 2002 to 2007. He is now an Associate Professor with Yeditepe University, Istanbul, Turkey, and adjunct Senior Research Scientist at Radar and Sensors Division of TUBITAK, Kocaeli, Turkey. He is also consultant to several national and international companies.